DRUG DELIVERY
2022, VOL. 29, NO. 1, 2815–2823
https://doi.org/10.1080/10717544.2022.2118401

Taylor & Francis
Taylor & Francis Group

RESEARCH ARTICLE

Acute myocardial infarction therapy using calycosin and tanshinone co-loaded; mitochondrion-targeted tetrapeptide and cyclic arginyl-glycyl-aspartic acid peptide co-modified lipid-polymer hybrid nano-system: preparation, characterization, and anti myocardial infarction activity assessment

Jieke Yan[a], Jing Guo[b], Yuzhen Wang[c], Xiaowei Xing[d], Xuguang Zhang[d], Guanghao Zhang[d] and Zhaoqiang Dong[d]

[a]Department of Renal Transplantation, The Second Hospital of Shandong University, Ji'nan, Shandong Province, PR China; [b]Department of Gynaecology, The Second Hospital of Shandong University, Ji'nan, Shandong Province, PR China; [c]Clinical Department, Jinan Vocation College of Nursing, Ji'nan, Shandong Province, PR China; [d]Department of Cardiology, The Second Hospital of Shandong University, Ji'nan, Shandong Province, PR China

ABSTRACT

Acute myocardial infarction (AMI) is one of the most common ischemic heart diseases. However, lack of sufficient drug concentration (in the ischemic heart) is the major factor of treatment failure. It is urgent for researchers to engineer novel drug delivery systems to enhance the targeted delivery of cardioprotective agents. The aim of the present study was to investigate the anti-AMI ability of calycosin (CAL) and tanshinone (TAN) co-loaded; mitochondrion-targeted tetrapeptide (MTP) and cyclic arginyl-glycyl-aspartic acid (RGD) peptide co-modified nano-system.: We prepared CAL and TAN combined lipid-polymer hybrid nano-system, and RGD was modified to the system to achieve RGD-CAL/TAN NS. MTP-131 was conjugated with PEG and modified onto the nanoparticles to achieve dual ligands co-modified MTP/RGD-CAL/TAN NS. The physicochemical properties of nano-systems were characterized. The AMI therapy ability of the systems was investigated in AMI rats' model. The size of MTP/RGD-CAL/TAN NS was 170.2 ± 5.6 nm, with a surface charge of −18.9 ± 1.9 mV. The area under the curve (AUC) and blood circulation half-life ($T_{1/2}$) of MTP/RGD-CAL/TAN NS was 178.86 ± 6.62 μg·min/mL and 0.47 h, respectively. MTP/RGD-CAL/TAN NS exhibited the most significant infarct size reduction effect of 22.9%. MTP/RGD-CAL/TAN NS exhibited the highest heart accumulation and best infarct size reduction effect, which could be used as a promising system for efficient treatment of cardiovascular diseases.

ARTICLE HISTORY
Received 19 July 2022
Revised 17 August 2022
Accepted 21 August 2022

KEYWORDS
Acute myocardial infarction; calycosin; tanshinone; lipid-polymer hybrid nano-system

Introduction

Acute myocardial infarction (AMI) is one of the most deadest diseases, with more than 7 million individuals worldwide each year and increasing number of patients year by year (Reed et al., 2017; Benjamin et al., 2018, 2019). The size of myocardial infarction (MI) is one of the strongest predictors of mortality following AMI, and an intensive investigation effort has been dedicated to novel therapies for reducing MI size (Mendez-Fernandez et al., 2020). However, lack of sufficient drug concentrations (low bioavailability) in the ischemic heart is the major factor of treatment failure. It is urgent for researchers to engineer novel drug delivery systems to enhance the targeted delivery of cardioprotective agents.

Polyethylene glycol (PEG) conjugated nanoparticles have been verified as promising drug delivery carriers for their enhanced permeability and retention (EPR) effect in ischemic myocardium, for their reduced uptake of the reticuloendothelial system (RES) in the liver and spleen and increased delivery of agents to MI zone (Lukyanov et al., 2004; Gao et al., 2013; Li et al., 2018). PEG, the highly flexible and hydrophilic polymer, is coated on the out-layer of nanocarriers such as liposomes, micelles, polymeric nanoparticles, lipid nanoparticles, etc., thus bringing prolonged drug circulation (Suk et al., 2016; Ou et al., 2021). With continuous using of targeted nanocarriers, extraordinary efforts have been focused on the development of mitochondria targeted drug delivery system for improving the therapeutic efficacy of AMI and minimizing the side effects (Bonora et al., 2019).

Mitochondria is a major intracellular organelle and an important drug intracellular target, which has functional roles in cellular metabolism, cell proliferation and death (Dhanasekaran et al., 2020). A mitochondrion-targeted

CONTACT Zhaoqiang Dong zhaoqiangdongsdu@outlook.com Department of Cardiology, The Second Hospital of Shandong University, Ji'nan, 250033, Shandong Province, PR China.

tetrapeptide, MTP-131 (also called elamipretide, SS-31, or Bendavia), H-D-Arg-Dmt-Lys-Phe-NH_2, is a water-soluble tetra-peptide (Miyamoto et al., 2020). It binds with high affinity to cardiolipin (CL), an anionic phospholipid expressed on the inner mitochondrial membrane that is required for cristae formation (Zhao et al., 2004; Birk et al., 2013). The mitochondria-targeted nanoparticles were developed to penetrate through the mitochondrial membrane, driving the molecules to accumulate within the mitochondria (Li et al., 2019). Hence, mitochondria-targeted drug delivery systems have achieved promising anticancer effects in cancer chemotherapy. Cyclic arginyl-glycyl-aspartic acid (RGD) peptide has been explored by our group as an $\alpha_v\beta_3$ integrin receptor-specific targeting moiety for the targeted delivery of nanoparticles to MI site, in which $\alpha_v\beta_3$ integrin is highly expressed (Dong et al., 2017).

Chinese herbal medicine (CHM) is more and more used in the treatment of AMI because of its good curative effect and less side effects, among which Radix astragali (Fabaceae astragalus propinquus Schischkin) is used in the preparation to treat AMI (Zhang et al., 2019). Calycosin (CAL) is the major bioactive chemical in the dry root extract of this medical plant (Gao et al., 2014). Tanshinone (TAN) is one of the key lipophilic components from the hemorheologic agent *Salvia miltiorrhiza bunge* in China and was used by our group to develop nanoparticles for AMI treatment (Guo et al., 2019).

Combination therapy AMI has been reviewed by Keeley et al. (Keeley & Weaver, 1999). It is a promising strategy because the synergistic effects could reduce systemic toxicity and at the same time, improve the therapeutic effects. Examples included Qiu et al developed a salvianolic acid B and panax notoginsenoside loaded nanomedicine for the combination therapy of AMI (Qiu et al., 2017). In the present research, RGD modified, CAL and TAN combined lipid-polymer hybrid nano-systems were prepared and MTP-131 was conjugated with PEG and modified to the nanoparticles for the targeted delivery to MI site (Figure 1). AMI therapy ability of the systems was investigated in AMI rats' model.

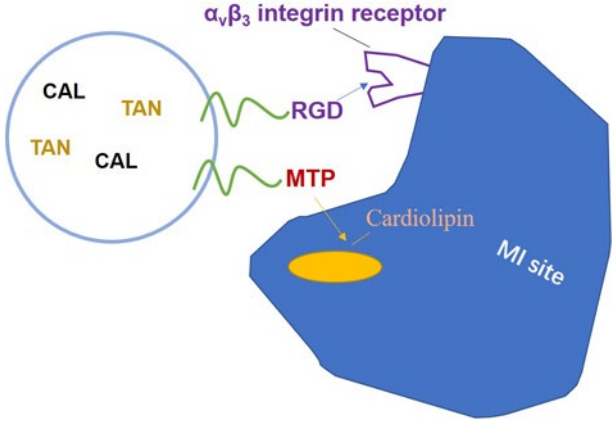

Figure 1. A schematic diagram of the nano formulation to reflect the mechanism of dual targeting.

Materials and methods

Materials

1,2-distearoyl-sn-glycero-3-phosphoethanolamine-N-[carboxy(polyethylene glycol)] (DSPE-PEG-COOH) was purchased from Ponsure Biotechnology Co., Ltd (Shanghai, China). Soybean lecithin (for injection) was provided by Nanjing Well Pharmaceutical Co., Ltd (Nanjing, China). Calycosin (CAL), Tanshinone IIA (TAN), Tween®80, Dulbecco's Modified Eagle's Medium (DMEM), and 3-[4, 5-dimethylthiazol-2yl]-2, 5 diphenyltetrazolium (MTT) were acquired from Sigma-Aldrich (St. Louis, MO). Injectable soya lecithin (ISL) was purchased from Shanghai Taiwei Pharmaceutical Co, Ltd (Shanghai, China). Fetal bovine serum (FBS) was obtained from Fisher Chemicals (Fairlawn, NJ).

Cells and animals

Human cardiac myocytes (HCM) were obtained from the American type culture collection (ATCC, Manassas, VA, USA). Male Sprague-Dawley (SD) rats (240–260 g) were obtained from the Center of Experimental Animals of Shandong Province (China). All the animal experiments conformed to the guidelines of the National Act on the Use of Experimental Animals (People's Republic of China) and the animal experiments were approved by the Medical Ethics Committee of the Second Hospital of Shandong University.

Preparation of CAL and TAN combined nano-system

CAL and TAN combined lipid-polymer hybrid nano-system (CAL/TAN NS) was prepared by nanoprecipitation method (Liu et al., 2018). DSPE-PEG-COOH (254 mg) and ISL (178 mg) were dispersed in distilled water to form the aqueous phase (A). PLGA (228 mg), CAL (30 mg), and TAN (30 mg) was dissolved in acetone to achieve organic phase (B). (B) was added dropwise into the (A) under stirring at a speed of 600 rpm until complete evaporation of the organic solvent (8 h) to get CAL/TAN NS. Single drug loaded nano-systems were prepared using CAL (60 mg) or TAN (60 mg) only, named CAL NS and TAN NS. To be noticed, in order to reduce the toxicity of drugs, the amounts of drugs in combined nano-system were reduced to half compared with single drug-loaded nano-system.

RGD modified, CAL and TAN co-loaded, lipid-polymer hybrid nano-system (RGD-CAL/TAN NS) was prepared using RGD-PEG-DSPE (298 mg) along with DSPE-PEG-COOH. RGD modified, blank NS (RGD NS) was also prepared using no drug.

Preparation of MTP-131 modified nano-system

CAL/TAN NS (200 mg) was dissolved in DMF (10 mL), EDC (20.0 mg) and NHS (12.0 mg) were added at 0 °C to activate the carboxylic acid groups of DSPE-PEG-COOH (A) (Jiang et al., 2021). Then MTP-131 (H-D-Arg-Dmt-Lys-Phe-NH_2) was

dissolved in DMF (5 mL) and added dropwise to the above (A) and stirred for 24 h. The resulting solution was dialyzed (MWCO = 2 kDa) against distilled water for 24 h to get MTP-131 modified CAL/TAN NS (MTP-CAL/TAN NS). MTP-131 and RGD co-modified, CAL and TAN co-loaded, lipid-polymer hybrid nano-system (MTP/RGD-CAL/TAN NS) was prepared using RGD-CAL/TAN NS (200 mg) instead of CAL/TAN NS (200 mg). MTP-131 was also reacted with RGD NS to prepare MTP-131 and RGD co-modified NS (MTP/RGD NS).

Characterization of nano-systems

To confirm the conjugation of MTP to CAL/TAN NS, the resident content of MTP in supernatant after reaction was quantified by HPLC (Kuang et al., 2017): the MTP-CAL/TAN NS mixture was centrifuged (13,000 g, 30 min) at 4 °C and the supernatant collected was mildly reduced by tris(2-carboxyethyl)phosphine hydrochloride (TECP) to generate free sulfhydryls. The analysis was performed using an HPLC system equipped with an RP-HPLC column (Inertsil ODS-SP C_{18} column, 5 μm, 4.6 mm × 250 mm). The parameters were as follows: flow rate, 1.0 ml/min; mobile phase A was 0.1% trifluoroacetic in acetonitrile, mobile phase B was 0.1% trifluoroacetic in water, wavelength and column temperature were set at 220 nm and 25 °C respectively.

The morphology of MTP/RGD-CAL/TAN NS and CAL/TAN NS was visualized using transmission electron microscope (JEOL, Tokyo, Japan) (Li et al., 2020). The particle size, size distribution and zeta potential were evaluated using dynamic light scattering (DLS) technique using a Zetasizer Nano ZS (Malvern Instruments, Malvern, UK). The CAL content in the NS was analyzed by HPLC method using a C18 column (250 mm × 4.6 mm, 5 μm) and the chromatogram was acquired at 254 nm (Liu et al., 2016). TAN content in the NS was measured by Sephadex-G25 column (15.0 × 1.5 cm^2) method using a UV5 ultraviolet spectrophotometer (Zhang et al., 2018). The encapsulation efficacy (EE) and drug loading (DL) were calculated using the following formula:

$$EE(\%) = \frac{\text{the amount of total drug-the amount of unentrapped drug}}{\text{the amount of total drug}} \times 100$$

$$DL(\%) = \frac{\text{the amount of total drug - the amount of unentrapped drug}}{\text{the amount of lipid + (the amount of total drug - the amount of unentrapped drug)}} \times 100$$

Stability and drug release

The serum stability of nano-systems was examined in phosphate buffers (PBS) solution contained 10% (v/v) fetal bovine serum (FBS) (Li et al., 2017). MTP/RGD-CAL/TAN NS and other NS were incubated with 10% FBS solution at 37 °C under 100 rpm gentle stirring for a period of 72 h. The size changes were monitored during this period. Drugs released from nano-systems was investigated using the dialysis method. MTP/RGD-CAL/TAN NS and other NS were sealed into dialysis bags (MWCO 10 KDa) and incubated in PBS (pH 7.4) at 37 °C with constant shaking at 100 rpm. During a period of 72 h, 0.5 mL of release media was extracted from the PBS at determined time points and the same volume of fresh buffer was added. Drugs released from nanoparticles were measured as described in 'Characterization of nano-systems' section.

In vitro cytotoxicity

In vitro cytotoxicity of nano-systems and free drugs were evaluated by MTT assay (Gao et al., 2017). HCM was seeded in 96-well plates (10^4 cells per well) and incubated for 24 h. MTP/RGD-CAL/TAN NS, MTP-CAL/TAN NS, CAL/TAN NS, CAL NS, TAN NS, and CAL/TAN solution at different concentrations were added to the cells and incubated for 48 h. Cells were washed with PBS for three times and treated with MTT solution (5 mg/mL), then maintained for another 4 h. The MTT medium was removed and the formazan crystals were dissolved by adding DMSO (200 μL) into each well. The relative cell viability is proportional to the absorbance observed at 570 nm with a Model 680 Microplate Reader (Bio-Rad Laboratories Inc., Hercules, CA, USA). The cytotoxicity of RGD-PEG-DSPE and MTP/RGD NS was also tested using the same method. Cell viability was calculated using the untreated cells as a control and according to the equation: Cell viability (%) = (absorbance of the sample − absorbance of the blank)/(absorbance of the control − absorbance of the blank) × 100.

Preparation of AMI model

AMI model was prepared by the permanent ligation of left coronary artery method as describe in our previous study (Dong et al., 2017). Briefly, 3.5 mL/kg of chloraldurate (10%, v/v) was intraperitoneal injected to the rats to anesthetize them. The heart was exteriorized, and ligated from the pulmonary conus to the left atrial appendage (2–3 mm). Then the heart was returned to its normal position, and the left thorax was sutured immediately. Sham-operated rats were subjected to the same surgical procedure without ligating the coronary artery.

In vivo pharmacokinetics and tissue distribution

AMI rats were randomly divided into five groups and received MTP/RGD-CAL/TAN NS, MTP-CAL/TAN NS, CAL/TAN NS, and CAL/TAN solution (10 mg CAL and TAN per kg of body weight via intravenous injection) (Zhang et al., 2016). Blood samples were obtained at determined times until 72 h after injection and 15 μL of heparin (1000 U/mL) was added to each sample, then the blood samples were immediately

centrifuged at 5000 rpm for 5 min at 4 °C and stored at −20 °C for further analysis. Rats were sacrificed at 2 h after injection, then tissues (heart, kidney, liver, spleen, and lung) were immediately harvested, homogenized and stored at −20 °C for further analysis (Yu et al., 2018). The drugs content was measured as described in 'Characterization of nano-systems' section.

In vivo effects on infarct size

AMI rats were randomly divided into six groups and received MTP/RGD-CAL/TAN NS (10 mg/kg CAL and 10 mg/kg TAN), MTP-CAL/TAN NS (10 mg/kg CAL and 10 mg/kg TAN), RGD-CAL/TAN NS (10 mg/kg CAL and 10 mg/kg TAN), CAL/TAN NS (10 mg/kg CAL and 10 mg/kg TAN), CAL NS (20 mg/kg CAL), TAN NS (20 mg/kg TAN), MTP/RGD NS, and CAL/TAN solution (10 mg/kg CAL and 10 mg/kg TAN), along with AMI group (received physiological saline) and sham-operated group (Shao et al., 2017). After 48 h of treatment, rats were sacrificed and the hearts were excised and sliced into 2-mm thick sections, then the slices were incubated in a solution of 1% 2,3,5-triphenyltetrazolium chloride (TTC) in phosphate buffered saline (pH 7.4) at 37 °C for 15 minutes (Yao et al., 2015). The infarct areas should be unstained, while normal myocardium areas were stained brick red. The infarct areas of hearts were calculated using Image J and calculated by the equation: Infarct size (%) = The size of the infarct area/the whole size of the left ventricle × 100.

Statistical analysis

Statistical analysis was performed by an unpaired t test between two groups, using SPSS version 21.0. Results were expressed as a mean ± standard deviation (SD). $^{*}P < .05$, $^{**}P < .01$ was considered statistically significant.

Results

Characterization of nano-systems

Figure 2 showed the preparation process of MTP-131 modified nano-system. The MTP-131 conjugation efficiency of MTP-CAL/TAN NS was calculated by HPLC analysis, which was determined to 79.5%. The size of MTP/RGD-CAL/TAN NS was 1170.2 ± 5.6 nm (Table 1), which is larger than that of CAL/TAN NS (122.5 ± 3.3 nm). After MTP modification, the surface charge of CAL/TAN NS (−31.4 ± 2.4 mV) reduced to −21.3 ± 2.3 mV (MTP-CAL/TAN NS). MTP/RGD-CAL/TAN NS and CAL/TAN NS showed uniform and spheroidal particles, the former one was observed to have some coats on the surface (Figure 3).

Stability and drug release

Stability of NS groups was evaluated by measuring the size changes, which were presented in Figure 4(A). The size showed no obvious change during 72 in the serum, which could prove the stability of NS in serum. The NLC was also stable without the presence of serum. Drug release from MTP/RGD-CAL/TAN NS and MTP-CAL/TAN NS was slower compared with unmodified CAL/TAN NS, which was presented in Figure 4(B) and 4(C).

In vitro cytotoxicity

Figure 5 showed the cytotoxicity of drug loaded NS and drug solution. Blank MTP/RGD NS and RGD-PEG-DSPE groups showed over 85% of cell viability. In contrast, drugs contained formulations exhibited cytotoxicity to some extent. The cytotoxicity of drugs loaded NS formulations was lower compared with CAL/TAN solution ($P < .05$), which could prove the protection effects of NS systems that could be used safely.

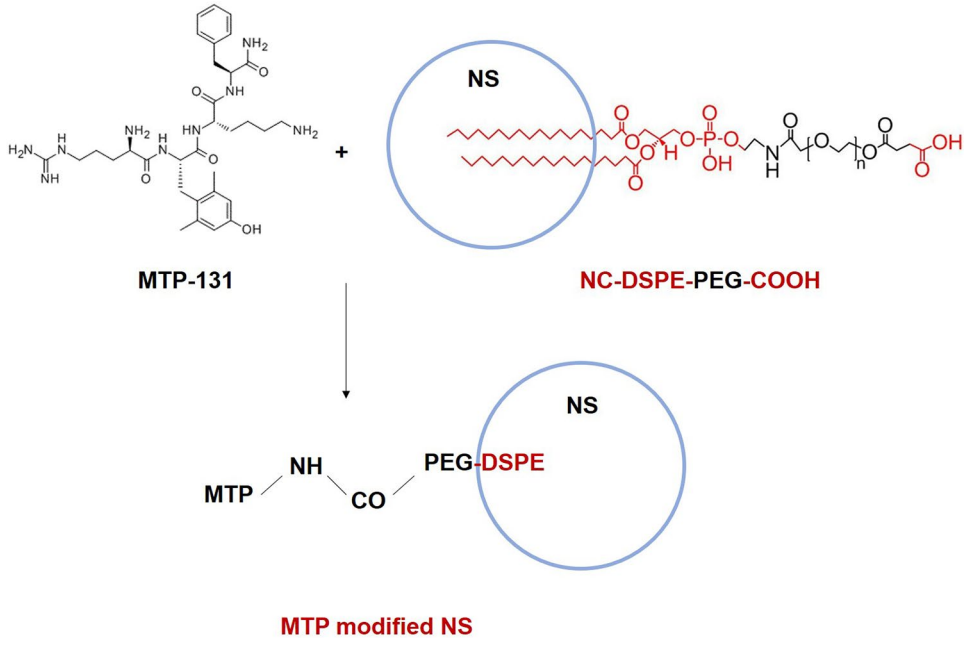

Figure 2. A scheme of the preparation of MTP-131 modified nano-system.

Table 1. Characterization of nano-systems.

Systems	Mean diameter (nm)	PDI	Zeta potential (mV)	EE (%)		DL (%)	
				CAL	TAN	CAL	TAN
MTP/RGD-CAL/TAN NS	170.2 ± 5.6	0.27 ± 0.04	−18.9 ± 1.9	82.1 ± 3.2	82.9 ± 2.8	9.1 ± 0.5	7.3 ± 0.4
MTP-CAL/TAN NS	168.7 ± 5.1	0.28 ± 0.05	−21.3 ± 2.3	81.3 ± 3.5	83.7 ± 3.1	9.5 ± 0.6	7.9 ± 0.5
RGD-CAL/TAN NS	123.9 ± 3.7	0.25 ± 0.04	−26.3 ± 2.2	81.5 ± 3.1	80.9 ± 3.2	8.9 ± 0.6	7.3 ± 0.5
CAL/TAN NS	122.5 ± 3.3	0.22 ± 0.03	−31.4 ± 2.4	80.4 ± 2.9	82.2 ± 3.4	8.8 ± 0.7	7.4 ± 0. 6
CAL NS	119.8 ± 3.5	0.24 ± 0.04	−30.3 ± 2.7	82.5 ± 3.4	N/A	9.1 ± 0.8	N/A
TAN NS	120.3 ± 3.1	0.21 ± 0.03	−29.5 ± 2.5	N/A	80.9 ± 3.6	N/A	8.1 ± 0.4
MTP/RGD NS	163.2 ± 4.8	0.25 ± 0.04	−20.5 ± 2.1	N/A	N/A	N/A	N/A
RGD NS	121.7 ± 2.9	0.19 ± 0.02	−32.5 ± 2.3	N/A	N/A	N/A	N/A

Data were expressed as a mean ± standard deviation (SD).

In vivo pharmacokinetics and tissue distribution

The drug concentration profiles in the blood were presented in Figure 6. For CAL profiles (Figure 6A), the area under the curve (AUC) of MTP/RGD-CAL/TAN NS was 178.86 ± 6.62 μg·min/mL, which is higher than that of MTP-CAL/TAN NS (126.71 ± 4.31 μg·min/mL) and CAL/TAN NS (101.3 ± 3.17 μg·min/mL) and CAL/TAN solution (41.75 ± 2.15 μg·min/mL). The blood circulation half-life ($T_{1/2}$) of MTP/RGD-CAL/TAN NS, MTP-CAL/TAN NS, CAL/TAN NS, and CAL/TAN solution was 8.22, 4.59, 2.13 and 0.47 h. The tissue distribution behaviors of drug contained NS and drug solution were evaluated on AMI rats (Figure 7). MTP/RGD-CAL/TAN NS illustrated the highest drug distribution in the heart, higher than MTP-CAL/TAN NS, CAL/TAN NS and CAL/TAN solution ($P < .05$). CAL/TAN solution exhibited a higher distribution in the kidney compared with NS formulations ($P < .05$).

In vivo AMI therapy

The infarct size changes were monitored to evaluate the *in vivo* anti AMI effects of drug contained NS and drug solution samples (Figure 8). The infarct size of blank MTP/RGD NS and AMI groups were 66.3%, and 67.1%, respectively. MTP/RGD-CAL/TAN NS exhibited the most significant infarct size reduction effect (22.9%), which was higher compared with MTP-CAL/TAN NS group (33.4%, $P < .05$). The infarct size of CAL/TAN NS group was 43.1%, which is larger than MTP-CAL/TAN NS, while smaller than that of CAL NS, TAN NS and CAL/TAN solution ($P < .05$). Dual drugs loaded CAL/TAN NS showed better *in vivo* AMI therapy effect compared with single drug loaded CAL NS and TAN NS.

Discussion

In the present research, CAL and TAN combined lipid-polymer hybrid nano-systems were prepared using PLGA as the polymeric core and DSPE-PEG as the lipid shell. PLGA is a negatively charged polymer. The negative zeta potential of CAL/TAN NS (−31.4 mV) could be the contribution of PLGA (Zhang et al., 2018). After MTP and RGD modification, the surface charge of was neutralized to −18.9 mV (MTP/RGD-CAL/TAN NS). Talk about ligands modification, there are two patterns: pre- and post-modification (Jian et al., 2020). Peeters et al argued that post-modified lipoplexes are better vehicles compared with pre-modified carriers (Peeters et al., 2007). Du and Li concluded that post-modified nanostructured lipid

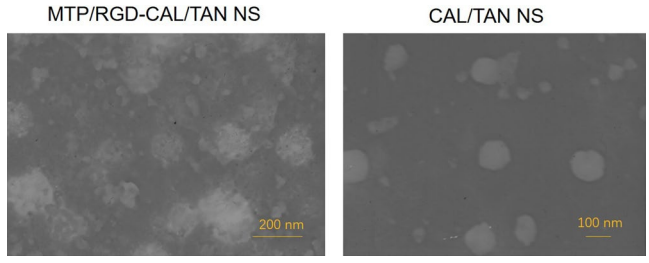

Figure 3. The TEM images of MTP/RGD-CAL/TAN NS and CAL/TAN NS.

carriers performed better than pre-modified ones for targeted lung cancer combination therapy (Du & Li, 2016). So in this study, MTP-131 was post-modified onto the nanoparticles after the CAL/TAN NS was prepared.

The size showed no obvious change during 72 in the serum, which could prove the stability of NS in serum with no aggregation occurred for the period of administration. This may contribute to the maintenance of colloidal stability even in serum-included media (Wang et al., 2018). Drug release from MTP/RGD-CAL/TAN NS was slower compared with unmodified CAL/TAN NS, which may be due to the MTP coating on the surface that hindered the drug release (Yang et al., 2018). The sustained release behavior of the NS could be explained by the lipid shell on the outside of the polymer core could also protect the drugs and let them release in a more sustained behavior (Fan et al., 2021). *In vitro* drug release of the drug loaded NS may be controlled by the diffusion, erosion and/or corrosion process, so that NS could achieve drug depot effects and lead to the sustained release of hydrophobic drugs (Guo et al., 2019).

Compared to other biomaterials, lipids offer advantages such as biocompatibility, biodegradability, limited toxicity and immunogenicity (Campani et al., 2016). Blank MTP/RGD NS group showed a cell viability of above 85%, in the meantime, the cytotoxicity of drugs loaded NS formulations was lower compared with CAL/TAN solution. These could be the evidence of the low toxicity of the nano-materials used in the system. Lower cytotoxicity could prove the fine protects effects of LPNs and well cytocompatibility of the nanoparticle formulations, which may benefit the use of them *in vivo*.

In vivo tissue distribution of NS was higher compared to CAL/TAN solution. This phenomenon could be due to the enhanced permeability and retention (EPR) effect in ischemic tissues, which is the primary mechanism of accumulation of passive targeting nanoparticles in the infarct areas (Frangogiannis et al., 2002). It was reported that PEG

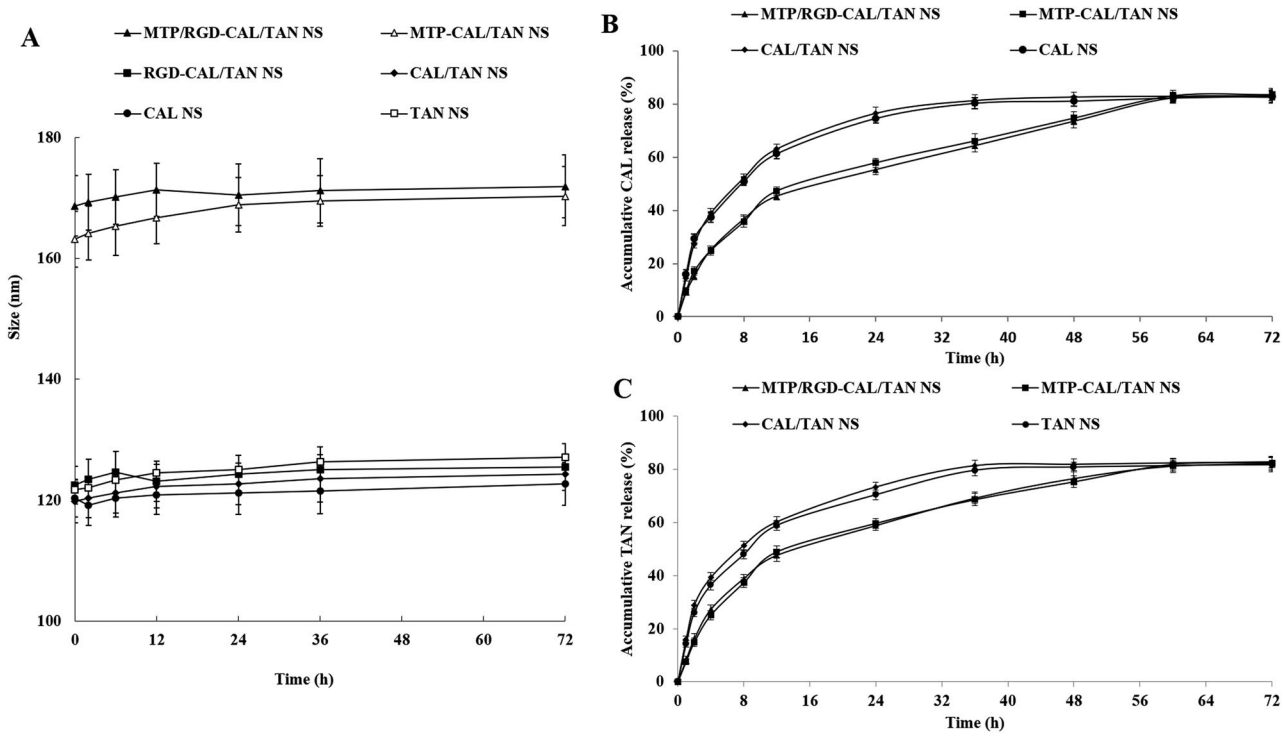

Figure 4. The serum stability of nano-systems examined in PBS solution contained 10% (v/v) FBS (A). CAL (B) and TAN (C) release from nano-systems investigated using the dialysis method.

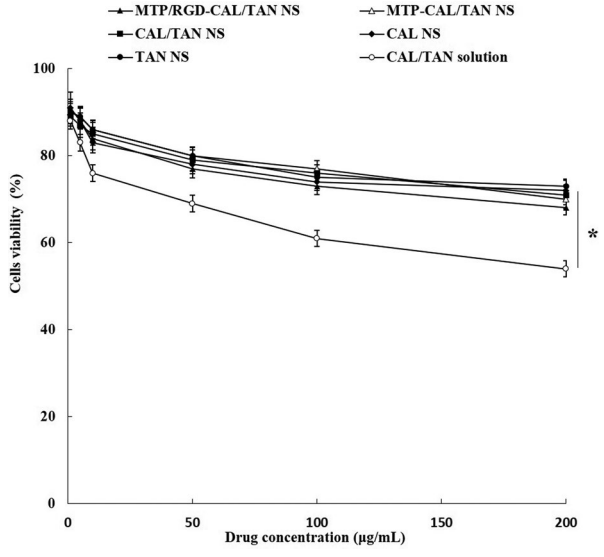

Figure 5. *In vitro* cytotoxicity of nano-systems and free drugs evaluated by MTT assay (* means $P < .05$).

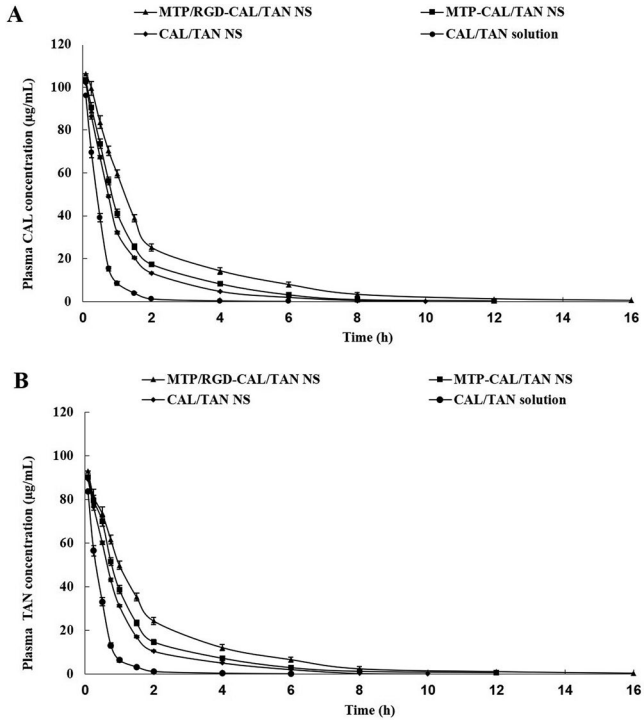

Figure 6. Plasma CAL (A) and TAN (B) concentrations of vs. time after i.v. administration of different formulations.

modification could help nanoparticles to escape from phagocytosis and capture by various organs, so that PEGylated nanoparticles had a longer circulation *in vivo* compared with naked nanoparticles (Sims et al., 2019). *In vivo* pharmacokinetics and tissue distribution in this study showed long-circulating characteristics of NS, which proved that NS system prolonged circulation time of drug and has great potential to accumulate in the myocardial infarct area (He et al., 2011). Higher heart distribution of MTP/RGD-CAL/TAN NS compared with CAL/TAN NS could be attributed to the ligands mediated targeting of modified nano-system (Pawar et al., 2016).

In vivo infarct therapy effect was evaluated by measuring the infarct size, which is considered to be a critical indicator to evaluate the cardiac damage (Ramachandra et al., 2020). Coronary artery ligation is a widely used method to establish the AMI rat model for the evaluation of the in vivo infarct

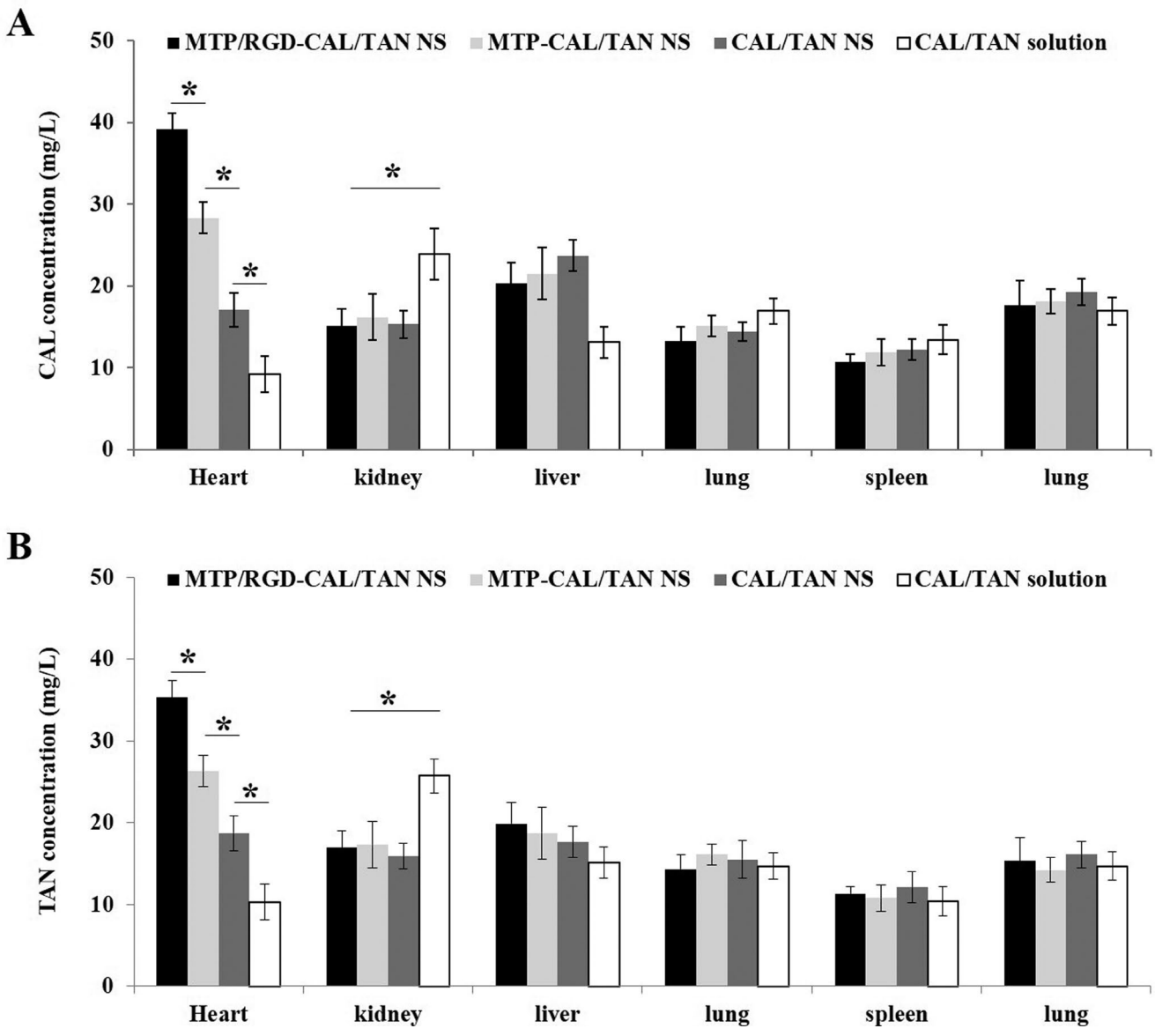

Figure 7. Tissue distribution of CAL (A) and TAN (B) after i.v. administration (* means $P < .05$).

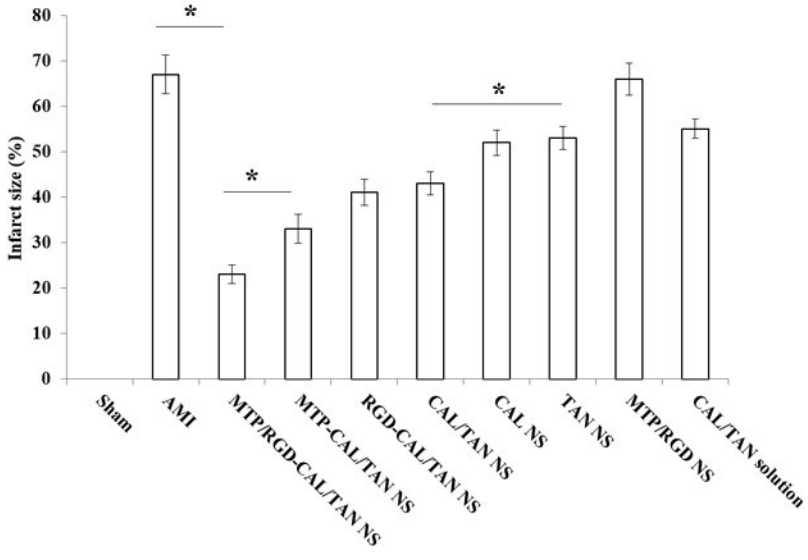

Figure 8. *In vivo* effects on infarct size when different formulations were used (* means $P < .05$).

therapy effect, because it is more clinically relevant to imitate the clinical status of patients (Agbo et al., 2019). MTP/RGD-CAL/TAN NS exhibited better infarct size reduction effect compared with MTP-CAL/TAN NS and CAL/TAN NS, suggesting the modification effect of the double modification of MTP-131 and RGD peptide. Dual drugs loaded CAL/TAN NS showed better AMI therapy effect compared with single drug loaded CAL NS and TAN NS, which could prove the synergistic effect of the two drugs when co-loaded in one system.

Conclusion

MTP/RGD-CAL/TAN NS could be used as a heart-targeted and long-circulated nano-system due to the targeted ligands and dual drugs loaded nanoparticles. MTP/RGD-CAL/TAN NS exhibited more heart accumulation and better infarct size reduction effect compared with MTP-CAL/TAN NS and CAL/TAN NS, suggesting the modification effect of the double ligands: MTP-131 and RGD peptide. *In vivo* infarct therapy studies in rats proved that dual drugs co-loaded NS showed better AMI therapy effect compared with single drug loaded NS. In summary, MTP/RGD-CAL/TAN NS was a promising system for efficient treatment of cardiovascular diseases.

Disclosure statement

The authors do not have any conflict of interest to declare.

Funding

The author(s) reported there is no funding associated with the work Q2 featured in this article.

References

Agbo E, Liu D, Li M, et al. (2019). Modulation of PTEN by hexarelin attenuates coronary artery ligation-induced heart failure in rats. Turk J Med Sci 49:945–58.

Benjamin EJ, Muntner P, Alonso A, et al. (2019). Heart disease and stroke statistics-2019 update: a report from the American Heart Association. Circulation 139:e56–e528.

Benjamin EJ, Virani SS, Callaway CW, et al. (2018). Heart disease and stroke statistics-2018 update: a report from the American Heart Association. Circulation 137:e67–e492.

Birk AV, Liu S, Soong Y, et al. (2013). The mitochondrial-targeted compound SS-31 re-energizes ischemic mitochondria by interacting with cardiolipin. J Am Soc Nephrol 24:1250–61.

Bonora M, Wieckowski MR, Sinclair DA, et al. (2019). Targeting mitochondria for cardiovascular disorders: therapeutic potential and obstacles. Nat Rev Cardiol 16:33–55.

Campani V, Salzano G, Lusa S, De Rosa G. (2016). Lipid nanovectors to deliver RNA oligonucleotides in cancer. Nanomaterials (Basel) 6:131.

Dhanasekaran S, Venugopal D, Al-Dayan N, et al. (2020). Emerging insights into mitochondria-specific targeting and drug delivering strategies: recent milestones and therapeutic implications. Saudi J Biol Sci 27:3581–92.

Dong Z, Guo J, Xing X, et al. (2017). RGD modified and PEGylated lipid nanoparticles loaded with puerarin: formulation, characterization and protective effects on acute myocardial ischemia model. Biomed Pharmacother 89:297–304.

Du J, Li L. (2016). Which one performs better for targeted lung cancer combination therapy: pre- or post-bombesin-decorated nanostructured lipid carriers? Drug Deliv 23:1799–809.

Fan X, Wang T, Ji Z, et al. (2021). Synergistic combination therapy of lung cancer using lipid-layered cisplatin and oridonin co-encapsulated nanoparticles. Biomed Pharmacother 141:111830.

Frangogiannis NG, Shimoni S, Chang SM, et al. (2002). Evidence for an active inflammatory process in the hibernating human myocardium. Am J Pathol 160:1425–33.

Gao H, Liu J, Yang C, et al. (2013). The impact of PEGylation patterns on the in vivo biodistribution of mixed shell micelles. Int J Nanomed 8:4229–46.

Gao J, Liu ZJ, Chen T, Zhao D. (2014). Pharmaceutical properties of calycosin, the major bioactive isoflavonoid in the dry root extract of Radix astragali. Pharm Biol 52:1217–22.

Gao Z, Li Z, Yan J, Wang P. (2017). Irinotecan and 5-fluorouracil-co-loaded, hyaluronic acid-modified layer-by-layer nanoparticles for targeted gastric carcinoma therapy. Drug Des Devel Ther 11:2595–604.

Guo J, Xing X, Lv N, et al. (2019). Therapy for myocardial infarction: in vitro and in vivo evaluation of puerarin-prodrug and tanshinone co-loaded lipid nanoparticulate system. Biomed Pharmacother 120:109480.

Guo S, Zhang Y, Wu Z, et al. (2019). Synergistic combination therapy of lung cancer: cetuximab functionalized nanostructured lipid carriers for the co-delivery of paclitaxel and 5-Demethylnobiletin. Biomed Pharmacother 118:109225.

He Q, Zhang Z, Gao F, et al. (2011). In vivo biodistribution and urinary excretion of mesoporous silica nanoparticles: effects of particle size and PEGylation. Small 7:271–80.

Jian X, Li S, Feng Y, et al. (2020). Influence of synthesis methods on the high-efficiency removal of Cr(VI) from aqueous solution by Fe-modified magnetic biochars. ACS Omega 5:31234–43.

Jiang T, Ma S, Shen Y, et al. (2021). Topical anesthetic and pain relief using penetration enhancer and transcriptional transactivator peptide multi-decorated nanostructured lipid carriers. Drug Deliv 28:478–86.

Keeley EC, Weaver WD. (1999). Combination therapy for acute myocardial infarction. J Am Coll Cardiol 34:1963–5.

Kuang X, Zhou S, Guo W, et al. (2017). SS-31 peptide enables mitochondrial targeting drug delivery: a promising therapeutic alteration to prevent hair cell damage from aminoglycosides. Drug Deliv 24:1750–61.

Li D, Cui R, Xu S, Liu Y. (2020). Synergism of cisplatin-oleanolic acid co-loaded hybrid nanoparticles on gastric carcinoma cells for enhanced apoptosis and reversed multidrug resistance. Drug Deliv 27:191–9.

Li S, Wang L, Li N, et al. (2017). Combination lung cancer chemotherapy: design of a pH-sensitive transferrin-PEG-Hz-lipid conjugate for the co-delivery of docetaxel and baicalin. Biomed Pharmacother 95:548–55.

Li W, Wu J, Zhang J, et al. (2018). Puerarin-loaded PEG-PE micelles with enhanced anti-apoptotic effect and better pharmacokinetic profile. Drug Deliv 25:827–37.

Li WQ, Wu JY, Xiang DX, et al. (2019). Micelles loaded with puerarin and modified with triphenylphosphonium cation possess mitochondrial targeting and demonstrate enhanced protective effect against isoprenaline-induced H9c2 cells apoptosis. Int J Nanomed 14:8345–60.

Liu J, Cheng H, Han L, et al. (2018). Synergistic combination therapy of lung cancer using paclitaxel- and triptolide-coloaded lipid-polymer hybrid nanoparticles. Drug Des Devel Ther 12:3199–209.

Liu L, Leng J, Yang X, et al. (2016). Rapid screening and identification of BSA bound ligands from radix astragali using BSA immobilized magnetic nanoparticles coupled with HPLC-MS. Molecules 21:1471.

Lukyanov AN, Hartner WC, Torchilin VP. (2004). Increased accumulation of PEG-PE micelles in the area of experimental myocardial infarction in rabbits. J Control Release 94:187–93.

Mendez-Fernandez A, Cabrera-Fuentes HA, Velmurugan B, et al. (2020). Nanoparticle delivery of cardioprotective therapies. Cond Med 3:18–30.

Miyamoto S, Zhang G, Hall D, et al. (2020). Restoring mitochondrial superoxide levels with elamipretide (MTP-131) protects *db/db* mice against progression of diabetic kidney disease. J Biol Chem 295:7249–60.

Ou LC, Zhong S, Ou JS, Tian JW. (2021). Application of targeted therapy strategies with nanomedicine delivery for atherosclerosis. Acta Pharmacol Sin 42:10–7.

Pawar H, Surapaneni SK, Tikoo K, et al. (2016). Folic acid functionalized long-circulating co-encapsulated docetaxel and curcumin solid lipid nanoparticles: in vitro evaluation, pharmacokinetic and biodistribution in rats. Drug Deliv 23:1453–68.

Peeters L, Sanders NN, Jones A, et al. (2007). Post-pegylated lipoplexes are promising vehicles for gene delivery in RPE cells. J Control Release 121:208–17.

Qiu J, Cai G, Liu X, Ma D. (2017). αvβ3 integrin receptor specific peptide modified, salvianolic acid B and panax notoginsenoside loaded nanomedicine for the combination therapy of acute myocardial ischemia. Biomed Pharmacother 96:1418–26.

Ramachandra CJA, Hernandez-Resendiz S, Crespo-Avilan GE, et al. (2020). Mitochondria in acute myocardial infarction and cardioprotection. EBioMedicine 57:102884.

Reed GW, Rossi JE, Cannon CP. (2017). Acute myocardial infarction. Lancet 389:197–210.

Shao M, Yang W, Han G. (2017). Protective effects on myocardial infarction model: delivery of schisandrin B using matrix metalloproteinase-sensitive peptide-modified, PEGylated lipid nanoparticles. Int J Nanomed 12:7121–30.

Sims LB, Curry KC, Parupalli S, et al. (2019). Efficacy of surface-modified PLGA nanoparticles as a function of cervical cancer type. Pharm Res 36:66.

Suk JS, Xu Q, Kim N, et al. (2016). PEGylation as a strategy for improving nanoparticle-based drug and gene delivery. Adv Drug Deliv Rev 99:28–51.

Wang Z, Wei Y, Fang G, et al. (2018). Colorectal cancer combination therapy using drug and gene co-delivered, targeted poly(ethylene glycol)-ε-poly(caprolactone) nanocarriers. Drug Des Devel Ther 12:3171–80.

Yang F, Li A, Liu H, Zhang H. (2018). Gastric cancer combination therapy: synthesis of a hyaluronic acid and cisplatin containing lipid prodrug coloaded with sorafenib in a nanoparticulate system to exhibit enhanced anticancer efficacy and reduced toxicity. Drug Des Devel Ther 12:3321–33.

Yao C, Shi X, Lin X, et al. (2015). Increased cardiac distribution of mono-PEGylated Radix Ophiopogonis polysaccharide in both myocardial infarction and ischemia/reperfusion rats. Int J Nanomed 10: 409–18.

Yu J, Li W, Yu D. (2018). Atrial natriuretic peptide modified oleate adenosine prodrug lipid nanocarriers for the treatment of myocardial infarction: in vitro and in vivo evaluation. Drug Des Devel Ther 12:1697–706.

Zhang S, Li J, Hu S, et al. (2018). Triphenylphosphonium and D-α-tocopheryl polyethylene glycol 1000 succinate-modified, tanshinone IIA-loaded lipid-polymeric nanocarriers for the targeted therapy of myocardial infarction. Int J Nanomed 13:4045–57.

Zhang S, Wang J, Pan J. (2016). Baicalin-loaded PEGylated lipid nanoparticles: characterization, pharmacokinetics, and protective effects on acute myocardial ischemia in rats. Drug Deliv 23:3696–703.

Zhang Y, Wu J, Guo S, et al. (2019). The clinical efficacy and safety of the Chinese herbal medicine Astragalus (Huangqi) preparation for the treatment of acute myocardial infarction: a systematic review of randomized controlled trials. Medicine (Baltimore) 98:e15256.

Zhao K, Zhao GM, Wu D, et al. (2004). Cell-permeable peptide antioxidants targeted to inner mitochondrial membrane inhibit mitochondrial swelling, oxidative cell death, and reperfusion injury. J Biol Chem 279:34682–90.